A new triplet band system of C3: The 3Πg–3Πu transition

H. Sasada, T. Amano, C. Jarman, and P. F. Bernath

Citation: J. Chem. Phys. **94**, 2401 (1991); doi: 10.1063/1.460710
View online: http://dx.doi.org/10.1063/1.460710
View Table of Contents: http://jcp.aip.org/resource/1/JCPSA6/v94/i4
Published by the American Institute of Physics.

A new triplet band system of C_3: The $\tilde{b}\,^3\Pi_g$–$\tilde{a}\,^3\Pi_u$ transition

H. Sasada[a] and T. Amano
Herzberg Institute of Astrophysics, National Research Council, Ottawa, Canada K1A OR6
C. Jarman and P. F. Bernath
Department of Chemistry, University of Arizona, Tucson, Arizona 85721

(Received 21 August 1990; accepted 2 November 1990)

A triplet band system of C_3 has been observed for the first time in absorption with a distributed-feedback (DFB) diode laser spectrometer and in emission with a Fourier transform spectrometer at around 6500 cm^{-1}. The band has been assigned to the $\tilde{b}\,^3\Pi_g$–$\tilde{a}\,^3\Pi_u$ system, and the spectroscopic constants in both the upper and lower states have been determined. It is demonstrated that near-infrared DFB lasers are promising radiation sources for spectroscopy of unstable molecules.

I. INTRODUCTION

The history of the spectroscopy of C_3 goes back more than a century. Huggins[1] recorded a band spectrum at around 4000 Å from a comet. The same band system has been repeatedly studied in various comets since then.[2] McKellar[3] observed the band in cool carbon stars. Herzberg[4] reproduced the band system in the laboratory for the first time. However, the species responsible for the band spectrum was not identified.

The first conclusive identification of the band system was achieved by Douglas[5] who observed the 4050 Å system in the laboratory at high resolution. The rotational constants for the upper and lower states were determined, and it was concluded that the C_3 molecule is linear both in the upper and lower states. Later, Gausset, Herzberg, Lagerqvist, and Rosen[6,7] made a more extensive and detailed analysis, and established the assignment of the transition to be $\tilde{A}\,^1\Pi_u$–$\tilde{X}\,^1\Sigma_g^+$. From the vibrational analysis, they found that the ν_2 vibrational frequency is very small ($\sim$63 cm^{-1}) in the ground state. In the upper electronic state, a large Renner–Teller effect was observed upon excitation of the bending vibration. From a detailed analysis, the bending vibrational frequency and the Renner–Teller parameter were determined.[7] Subsequently, Merer[8] extended the analysis of the $\tilde{A}\,^1\Pi_u$–$\tilde{X}\,^1\Sigma_g^+$ system, and also found the ν_1 frequency in the ground state to be 1224.5 cm^{-1}.

More recently Lemire *et al.*[9] observed a new band system in 266–302 nm, but its assignment is uncertain. Rohlfing applied laser-induced fluorescence and dispersed-fluorescence spectroscopy to jet-cooled C_3[10] in the uv region, and observed a vibronically induced band system. In addition, two groups of workers[11,12] have used the technique of stimulated pumping from the $\tilde{A}\,^1\Pi_u$ to characterize higher vibrational levels of the ground state. These data will provide a very extensive description of the ground state potential surface.

The C_3 molecule also was a subject of extensive investigations in the visible and infrared regions using low temperature matrix isolation techniques. To our knowledge, the first report on the spectrum of the matrix isolated C_3 was published by Barger and Broida in 1962.[13] They deposited carbon vapor from the Knudsen cell at 2500 K, and recorded 21 "lines" in the range between 3797 and 4221 Å. Weltner and co-workers carried out extensive investigations on carbon vapor condensed in rare-gas matrices at 4 and 20 K.[14–16] In addition to the visible bands, they observed the infrared spectra of C_3 for the first time, and determined the ν_3 fundamental frequency to be 2040 cm^{-1}.[15] An important contribution from their work was the discovery of a long-lived (20 ms) emission band at around 5900 Å. They proposed that this band was the $\tilde{a}\,^3\Pi_u$–$\tilde{X}\,^1\Sigma_g^+$ system.[15] Bondybey and English[17] made additional observations of this phosphorescence. A vacuum UV spectrum of C_3 trapped in argon at 8 K was observed by Chang and Graham.[18] The status of the spectroscopy of matrix isolated C_3 and other carbon clusters was recently reviewed by Weltner and Van Zee.[19]

Matsumura *et al.*[20] generated C_3 by ArF excimer laser photolysis of diacetylene and observed the ν_3 fundamental band at around 2040 cm^{-1} in gas phase using diode laser spectroscopy. They also observed the $2\nu_2 + \nu_3$ combination band and various hot bands.[21] The ν_3 band of C_3 was simultaneously discovered in the circumstellar envelope of a giant carbon star IRC + 10216 by Hinkle, Keady, and Bernath.[22]

However, all the observations made so far concern the singlet states except for the 5900 Å emission system observed in low temperature matrices. Although Gausset *et al.*[7] obtained indirect evidence of a triplet state, stating that "there is some evidence for an $\tilde{a}\,^3\Pi_u$–$\tilde{X}\,^1\Sigma_g^+$ transition at larger wavelengths, and small perturbations in the main system are probably caused by the $^3\Pi_u$ state," no direct observation of the triplet band system has been reported so far. The lowest electron configuration is $\cdots(4\sigma_g)^2(3\sigma_u)^2(1\pi_u)$.[4] The low-lying triplet states arise from the electron configurations of $\cdots(4\sigma_g)^2(3\sigma_u)(1\pi_u)^4(1\pi_g)[^3\Pi_u, ^1\Pi_u]$ and $\cdots(4\sigma_g)(3\sigma_u)^2(1\pi_u)^4(1\pi_g)[^3\Pi_g, ^1\Pi_g]$. A number of *ab initio* calculations were carried out to obtain important information such as the molecular structure, the vertical excitation energies,[23–27] and the vertical electron affinity and ionization potential.[28] From these calculations, it is expected that the lowest triplet state lies about 2 eV higher than the ground state and the separation between this triplet state and the second triplet state is about 0.8 eV. Table I summarizes some of the recent calculated vertical energies of several excited states of C_3.

[a] Permanent address: Department of Physics, Faculty of Science and Technology, Keio University, 14-1, Hiyoshi 3-Chome, Kohoku-ku, Yokohama 223, Japan.

 0021-9606/91/042401-07$03.00

TABLE I. Calculated and observed excitation energies of C_3 (eV).

State	Configuration	EOM[a]	MRDCI[b]	CI[c]	FSMRCC[d] Basis I	FSMRCC[d] Basis II	Exp.
$\tilde{X}\,^1\Sigma_g^+$	$\cdots(4\sigma_g)^2(3\sigma_u)^2(1\pi_u)^4$	0.00	0.00	0.00	0.00	0.00	0.00
$\tilde{a}\,^3\Pi_u$	$\cdots(4\sigma_g)^2(3\sigma_u)(1\pi_u)^4(1\pi_g)$	1.73	2.11	2.13	2.09	2.07	2.10[e]
$\tilde{A}\,^1\Pi_u$		3.36	3.16	3.54	3.29	3.23	3.06[f]
$\tilde{b}\,^3\Pi_g$	$\cdots(4\sigma_g)(3\sigma_u)^2(1\pi_u)^4(1\pi_g)$	2.66	2.87		2.82	2.81	2.90[g]
$^1\Pi_g$		5.02	4.17		4.26	4.19	
$^3\Sigma_u^+$	$\cdots(4\sigma_g)^2(3\sigma_u)^2(1\pi_u)^3(1\pi_g)$	2.95	3.36	3.30	3.25	3.16	
$^3\Delta_u$		3.61	3.81	3.65	3.71	3.63	
$^3\Sigma_u^-$		4.07	4.04	3.90	4.06	4.01	
$^1\Sigma_u^-$		4.08	4.10	3.91	4.06	4.00	
$^1\Delta_u$		4.18	4.13	3.98	4.12	4.08	
$^1\Sigma_u^+$		7.68	8.14	9.48	8.03	7.76	6.6[h]

[a] Equations of motion method, Ref. 23.
[b] Multireference double-excitation configuration interaction method, Ref. 25.
[c] MCSCF calculation with limited configuration interaction, Ref. 28.
[d] Reference 27.
[e] References 15 and 17.
[f] Reference 7.
[g] This work, combined with the singlet–triplet splitting of Refs. 15 and 17.
[h] Reference 18.

In this paper, we report the first observation of a triplet–triplet band system at about 6500 cm^{-1} in gas phase, which has been assigned to the $\tilde{b}\,^3\Pi_g$–$\tilde{a}\,^3\Pi_u$ system. The band system has been obtained in absorption using a distributed-feedback (DFB) diode laser spectrometer and in emission using a Fourier-transform spectrometer. Figure 1 illustrates the locations of some low-lying excited states relevant to this work.

Near-infrared semiconductor lasers, originally developed for telecommunication with glass fiber networks, are also excellent sources for spectroscopy, although the frequency coverage is currently limited in relatively narrow regions around 1.3 and 1.5–1.6 μm. Despite the limited frequency coverage, the high sensitivity of spectrometer systems with these semiconductor lasers have already been demonstrated in high-resolution spectroscopy of overtone or combination bands of stable molecules.[29] Also recently the observation of the $2\nu_1$ band of HN_2^+ was reported.[30]

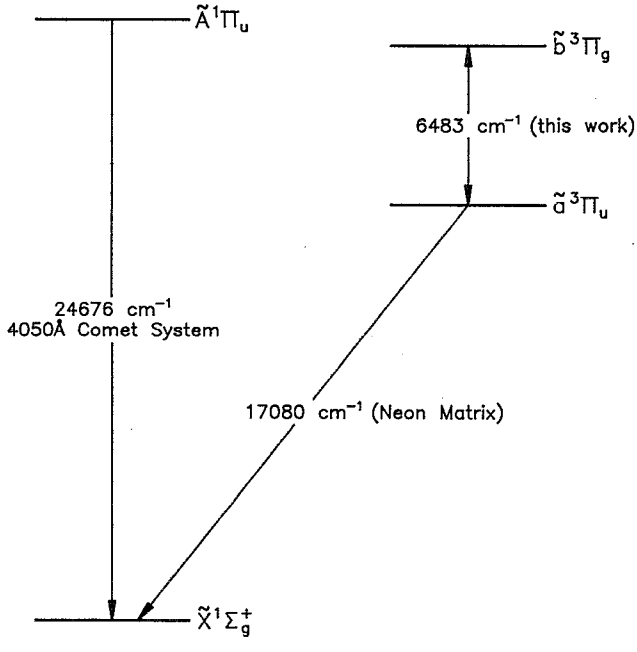

FIG. 1. The low-lying states of C_3.

II. EXPERIMENTAL TECHNIQUE

In the experiment conducted at National Research Council, Ottawa, DFB (distributed feedback) semiconductor lasers were used as radiation sources. DFB semiconductor lasers oscillate in a single longitudinal mode and the frequency can be scanned over 50 cm^{-1} without mode hops by changing the temperature. Several InGaAsP DFB semiconductor lasers (Hitachi HL1541A) were used in the present work. The temperature was controlled using a Peltier element. A 1.5 kHz small amplitude sinusoidal current was superposed to modulate the frequency. The output power which depends on the dc injection current was typically 5 mW at the injection current of 80 mA.

Radiation from the laser was divided into three beams with two beam splitters. The main beam was led into a hollow-cathode discharge cell fitted with a set of multitraversal mirrors. The effective absorption path length was 20 m. Details of the cell have been as described in one of our previous papers.[31] The transmitted power was detected by a germanium photodiode and the photocurrent was phase-sensitively detected by a lock-in amplifier at the discharge modulation frequency.

The second beam was steered through a 50 cm long absorption cell filled with 9 Torr of HCN ($H^{12}CN$ 80%, $H^{13}CN$ 20%) for the wave number calibration. The transition frequencies of the HCN lines were calibrated against the 1.52 μm He–Ne laser line.[32] The accuracy of the calibration HCN lines is about 30 MHz.

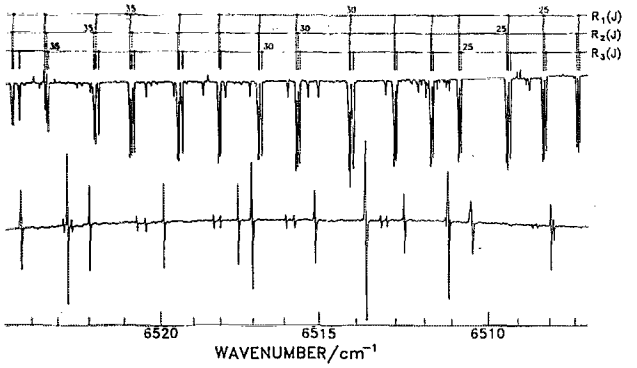

FIG. 2. A section of the absorption spectrum of the $\tilde{b}\,^3\Pi_g$–$\tilde{a}\,^3\Pi_u$ transition of C_3. The R_1, R_2, and R_3 notation denote the R branches for F_1, F_2, and F_3 components, respectively. The bottom trace represents the transitions of HCN used for frequency calibration.

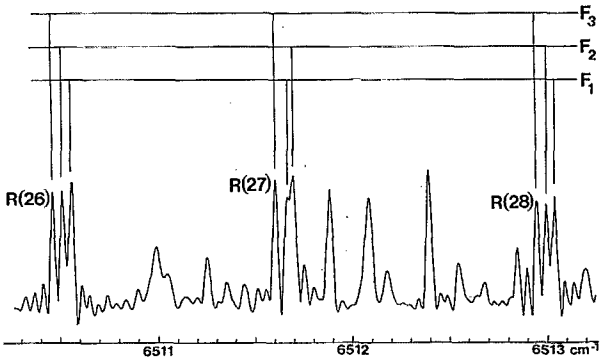

FIG. 4. A small section of the emission spectrum recorded with a Fourier-transform spectrometer. Here the N rotational quantum numbers are used rather than J.

The third beam was coupled to an etalon with 2.2 GHz free spectral range. The two beams used for recording the reference spectrum and the etalon fringes were monitored by two InSb photovoltaic detectors and the signals were demodulated using two lock-in amplifiers operated at the source modulation frequency. The outputs of the three lock-in amplifiers (C_3 signal, HCN lines, and the etalon fringes) were simultaneously recorded with a three-pen chart recorder.

Figure 2 shows a section of the absorption spectrum obtained from a hollow cathode discharge in 20 mTorr of propylene (C_3H_6) with about 1 Torr of He buffer. Essentially the same spectrum was obtained in the discharge of C_2H_2, C_2H_4, C_2H_6, or C_3H_4 with He buffers. The discharge in CH_4 also produced a similar spectrum, but the signal intensity was about one-third. The discharge in fully deuterated ethane yielded the same spectrum, which is evidence that the species does not contain hydrogen and contains only carbon atoms. Most of the spectra of C_3 were recorded using a discharge of 800 mTorr He and 15 mTorr C_2H_2 with the time constant of 40 ms.

A discharge modulation scheme was employed to enhance the sensitivity. High voltage alternating current supplied by an audio amplifier through a step-up transformer was applied to the anode. As a result, the concentration of molecules was modulated at the switching frequency of the discharge. The peak discharge current was 800 mA and the cathode was maintained at about -50 °C by flowing cooled methanol through copper tubing directly soldered onto the outer surface of the cathode.

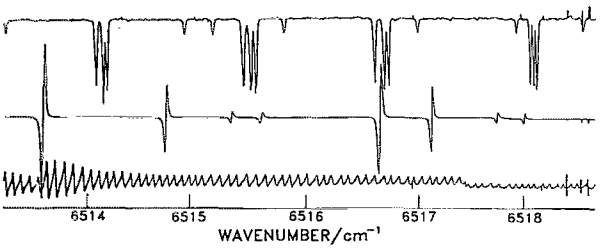

FIG. 3. A close up of the absorption spectrum shown in Fig. 2. The bottom trace shows the interference fringes from the etalon.

The modulation frequency was 10 kHz for most measurements in this work. The similar signal to noise ratio was attained at higher modulation frequencies up to about 15 kHz. With lower modulation frequencies, the noise increased while the signal intensity stayed constant. In the matrix spectra,[15,17] the phosphorescence from the $\tilde{a}\,^3\Pi_u$ state was found to have a lifetime of about 20 ms. The modulation frequency dependence of the signal intensity observed in this

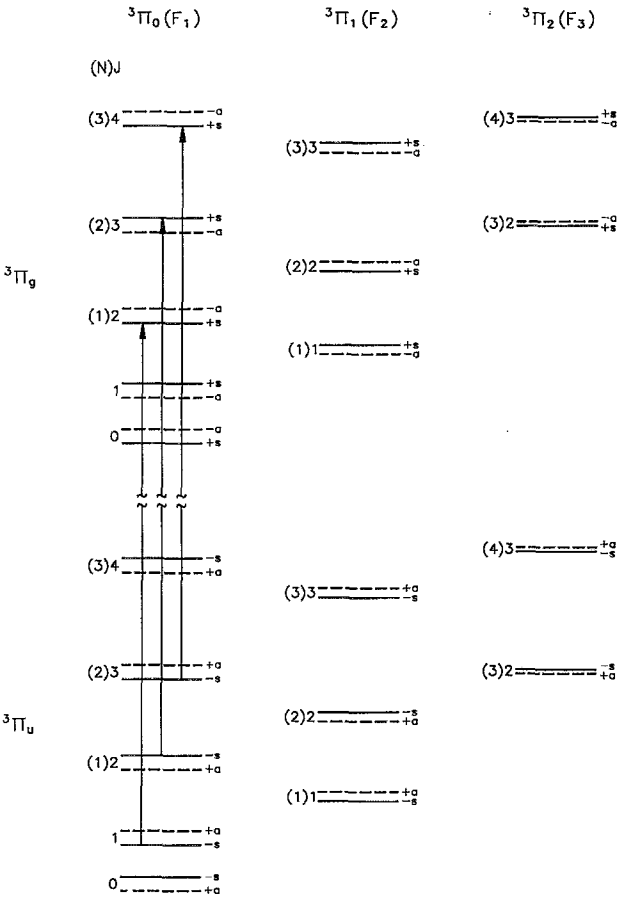

FIG. 5. A schematic energy level diagram of the lowest triplet states of C_3. The Λ-doubling splittings shown are exaggerated and are not to scale. Three representative R-branch transitions are shown by vertical arrows, which indicate the staggering in the rotational spacing due to the Λ doubling.

TABLE II. Observed wave numbers of the $\tilde{b}^3\Pi_g$–$\tilde{a}^3\Pi_u$ transition of C_3 (in cm^{-1}).

	$F_1(\Omega=0)$				$F_2(\Omega=1)$				$F_3(\Omega=2)$			
	P branch		*R* branch		*P* branch		*R* branch		*P* branch		*R* branch	
J'	Obs.	Δ[a]	Obs.	Δ	Obs.	Δ	Obs.	Δ	Obs.	Δ	Obs.	Δ
(A) *f* component												
1	6480.5460	35	6482.8910	63	6480.6437	−137[b]						
3	6479.0498	23	6484.5225	27	6479.0498	−51	6484.8539	20	6479.0498	−2731[b]	6485.2824	−2857[b]
5	6477.6045	33	6486.2207	18	6477.5443	30	6486.6589	2	6477.4361	−2494[b]	6487.2214	−2509[b]
7	6476.2028	12	6487.9869	16	6476.0791	−80	6488.5262	−57	6476.1454	229[b]	6489.4575	355[b]
									6475.7315[c]	−3910[b]	6489.0269[c]	−3951[b]
9	6474.8487	8	6489.8150	−51	6474.6807	−111[b]	6490.4515	−177[b]	6474.5602	−743[b]	6491.3422	−751[b]
11	6473.5367	−38	6491.7209	−30	6473.3352	−198[b]	6492.4459	−223[b]	6473.0925	−1282[b]	6493.3303	−1290[b]
13	6472.2760	−45	6493.6912	−41	6472.0422	−344[b]	6494.4850	−417[b]	6471.7253	−1534[b]	6495.3972	−1524[b]
15	6471.0684	−6	6495.7278	−44	6470.8126	−439[b]	6496.5974	−458[b]	6470.4133	−1927[b]	6497.4923	−1975[b]
17	6469.9056	−15	6497.8314	−16	6469.6273	−672[b]	6498.7493	−675[b]	6468.9394	−4609[b]	6499.4250	−4557[b]
									6469.9878[c]	5875[b]	6500.4726[c]	5918[b]
19	6468.7907	−44	6499.9976	20	6468.4478	−1423[b]	6500.9028	−1433[b]	6468.3577	990[b]	6502.2229	1001[b]
21	6467.7367	27	6502.2229	51	6467.7367	1940[b]	6503.5228	1920[b]	6467.2131	340[b]	6504.4529	369[b]
23	6466.7235	5	6504.4947	−25	6466.5950	439[b]	6505.7210	516[b]	6466.1756	166[b]	6506.7787	187[b]
25	6465.7608	−15	6506.8348	22	6465.6266	125[b]	6508.0747	137[b]	6465.2040	80	6509.1627	86
27	6464.8581	71	6509.2253	41	6464.7342	37	6510.5104	64	6464.2922	40	6511.6050	80
29	6463.9894	16	6511.6657	44	6463.8951	−35	6512.9907	−63	6463.4277	−54	6514.0761	−114
31	6463.1670	−41	6514.1429	−75	6463.1058	−106	6515.5303	−79	6462.6027	−253[b]	6516.5970	−269[b]
33	6462.3910	−86[b]	6516.6760	−105[b]	6462.3857	37	6518.1250	−5	6461.8401	−305[b]	6519.1648	−391[b]
35	6461.6602	−106[b]	6519.2446	−218[b]	6461.6823	−100[b]	6520.7400	−166[b]	6461.0656	−923[b]	6521.7306	−947[b]
37	6460.9476	−347[b]	6521.8536	−342[b]	6461.0353	−99[b]	6523.4248	−41[b]	6460.3100	−1768[b]	6524.3163	−1693[b]
39	6460.2832	−476[b]	6524.5026	−446[b]	6460.4294	−77[b]	6526.1277	−114[b]	6459.4553	−3982[b]	6526.7870	−3943[b]
41	6459.6141	−990[b]	6527.1437	−974[b]	6459.8490	−154[b]	6528.8688	−154[b]				
(B) *e* component												
0	6481.3330	−1										
2	6479.8051	5	6483.7290	−8	6479.8570	71			6479.9350	−2338[b]		
4	6478.3234	−44	6485.4016	−4	6478.3234	82	6485.7376	25			6486.2824	−2316[b]
6	6476.9003	−8	6487.1363	−16	6476.8327	−57	6487.5695	−54	6477.4361	5368[b]	6488.9847	5435[b]
8	6475.5240	2	6488.9430	28	6475.3925	−247[b]	6489.4575	−252[b]	6475.4909	1122[b]	6490.5218	1074[b]
10	6474.1972	17	6490.8080	−22	6474.0301	−211[b]	6491.4291	−253[b]	6473.8254	−1093[b]	6492.3237	−1113[b]
12	6472.9185	13	6492.7465	−20	6472.7042	−359[b]	6493.4472	−391[b]	6472.4158	−1502[b]	6494.3533	−1519[b]
14	6471.6897	4	6494.7490	−54	6471.4271	−575[b]	6495.5256	−500[b]	6471.0684	−2013[b]	6496.4178	−2089[b]
16	6470.5132	1	6496.8322	53	6470.2240	−604[b]	6497.6671	−529[b]	6470.4722	4287[b]	6499.2291	4285[b]
									6469.4423[c]	−6011[b]	6498.1954[c]	−6051[b]
18	6469.3925	35	6498.9657	16	6469.0649	−748[b]	6499.8490	−695[b]	6468.9395	548[b]	6501.0901	623[b]
20	6468.3577	403[b]	6501.1991	352[b]	6467.9358	−1140[b]	6502.0488	−1208[b]	6467.7997	91	6503.3151	67
22	6467.2945	−35[b]	6503.4212	−33[b]	6467.4524	4381[b]	6504.9155	4426[b]	6466.7562	−27	6505.6391	−27
					6466.5320[c]	−4823[c]	6503.9880[c]	−4848[b]				
24	6466.3105	−206[b]	6505.7210	−231[b]	6466.1068	747[b]	6506.9094	826[b]	6465.7809	−68	6508.0224	−54
26	6465.4095	−63	6508.1186	−18	6465.1391	371[b]	6509.2618	311[b]	6464.8674	−70	6510.4660	8
28	6464.5474	−35	6510.5572	57	6464.2319	94	6511.7004	176	6464.0146	−20	6512.9450	−77
30	6463.7295	−58	6513.0292	−55	6463.3919	1	6514.1779	−38	6463.2113	−8	6515.4851	−35
32	6462.9687	12	6515.5736	54	6462.6027	−54	6516.7130	−128	6462.4601	18	6518.0742	28
34	6462.2501	51	6518.1481	−8	6461.8401	−288[b]	6519.2811	−316[b]	6461.7554	32	6520.7080	97
36	6461.5747	89	6520.7737	−5	6461.1276	−442[b]	6521.8900	−502[b]	6461.0927	16	6523.3720	50
38	6460.9476	207[b]	6523.4706	292[b]	6460.4294	−842[b]	6524.5291	−761[b]	6460.4757	44	6526.0761	13
40	6460.3450	199[b]	6526.1703	239[b]	6459.7470	−1441[b]	6527.1538	−1509[b]	6459.8872	−22	6528.8104	−77
42	6459.7927	357[b]	6528.9145	284[b]	6459.0697	−2308[b]	6529.8108	−2245[b]				
44	6459.2641	458[b]	6531.7019	456[b]	6458.3671	−3704[b]	6532.4071	−3860[b]				
46			6534.5041	519[b]								
48	6458.2891	782[b]	6537.3225	533[b]								

[a] (Obs. − calc.) × 10^4.
[b] Excluded from fit.
[c] Perturbing line.

work suggests that the lifetime of the $\tilde{a}\ ^3\Pi_u$ state is much shorter, of the order of 50 μs, in the gas phase. Presumably, C_3 in the $\tilde{a}\ ^3\Pi_u$ state undergoes rapid collisional relaxations or is lost through chemical reactions with C_2H_2.

Accuracy of the measurements was typically about $\pm$ 0.003 cm^{-1}. The biggest source of this uncertainty was the uneven scan caused by the temperature scan controlled by a human being. This will be rectified in the future, and the measurement accuracy will be improved by a factor of 2 or so.

TABLE III. Derived combination differences for the $\tilde{a}\ ^3\Pi_u$ state (in cm^{-1}).

	$F_1(\Omega=0)$		$F_2(\Omega=1)$		$F_3(\Omega=2)$	
$J'-J''$	Obs.	Δ[a]	Obs.	Δ	OBs.	Δ
(A) f component						
2–0	2.3450	27				
4–2	5.4727	2	5.8041	71	6.2326	−125[b]
6–4	8.6162	−15	9.1146	−27	9.7853	−12
8–6	11.7841	4	12.4471	22	13.2954	−41
10–8	14.9663	−61	15.7708	−65	16.7820	−8
12–10	18.1842	8	19.1107	−25	20.2378	−8
14–12	21.4152	5	22.4428	−73	23.6719	8
16–14	24.6594	−37	25.7848	−18	27.0790	−47
18–16	27.9258	−2	29.1220	−1	30.4856	52
					30.4848[c]	44
20–18	31.2069	64	32.4550	−10	33.8652	11
22–20	34.4862	23	35.7861	−20	37.2398	28
24–22	37.7712	−30	39.1260	77	40.6031	20
26–24	41.0740	37	42.4481	13	43.9587	6
28–26	44.3672	−30	45.7762	27	47.3128	40
30–28	47.6763	27	49.0956	−27	50.6484	−61
32–30	50.9759	−33	52.4245	27	53.9943	−13
34–32	54.2850	−17	55.7393	−44	57.3247	−85
36–34	57.5844	−112	59.0577	−65	60.6650	−23
38–36	60.9060	5	62.3895	57	64.0063	74
40–38	64.2194	30	65.6983	−38	67.3317	38
42–40	67.5296	16	69.0198	0		
44–42			72.3222	−146[b]		
(B) e component						
3–1	3.9239	−13				
5–3	7.0782	40	7.4142	−57		
7–5	10.2360	−6	10.7368	2	11.5486	67
9–7	13.4190	25	14.0650	−5	15.0309	−47
11–9	16.6108	−38	17.3990	−44	18.4983	−20
13–11	19.8280	−35	20.7430	−32	21.9375	−17
15–13	23.0593	−58	24.0985	74	25.3494	−75
17–15	26.3190	51	27.4431	74	28.7569	−3
					28.7531[c]	−41
19–17	29.5732	−17	30.7841	53	32.1506	74
21–19	32.8414	−52	34.1130	−67	35.5154	−22
23–21	36.1267	2	37.4631	46	38.8829	1
			37.4560[c]	−25		
25–23	39.4105	−25	40.8026	77	42.2415	13
27–25	42.7091	43	44.1227	−60	45.5986	77
29–27	46.0098	92	47.4685	80	48.9304	−57
31–29	49.2997	2	50.7860	−40	52.2738	−27
33–31	52.6049	41	54.1103	−74	55.6141	10
35–33	55.8980	−60	57.4410	−28	58.9526	64
37–35	59.1990	−96[b]	60.7624	−59	62.2793	32
39–37	62.5230	85	64.0997	82	65.6004	−30
41–39	65.8253	38	67.4068	−67	68.9232	−54
43–41	69.1218	−74	70.7411	61	72.2667	146[b]
45–43	72.4378	−1	74.0400	−154[b]	75.5785	44
47–45	75.7489	12				
49–47	79.0334	−250[b]				

[a] (Obs. − calc.) × 10^4.
[b] Excluded from fit.
[c] Derived from the perturbing lines.

The $\tilde{b}\ ^3\Pi_g$–$\tilde{a}\ ^3\Pi_u$ emission was found in Fourier-transform spectra recorded for other purposes. These spectra were excited by an electrodeless microwave discharge of 2.75 Torr of He, 0.30 Torr of CH_4, and 0.040 Torr of white phosphorus vapor flowing in a 1/2 in. quartz tube. The phosphorus is presumably not required to produce C_3 but a discharge of 0.80 Torr of allene in 3.3 Torr argon did not show the C_3 emission spectra. The CH_4/P_4/He discharge was extremely rich with CO, CH, CP, P_2, C_2, as well as C_3. The PH, CP, CH, and C_2 work has been already published.[33–37]

The emission from the discharge tube was observed with the McMath Fourier-transform spectrometer of the National Solar Observatory at Kitt Peak. InSb detectors and a silicon filter limited the bandpass to approximately 1800–9000 cm^{-1}. The unappodized resolution was set to 0.02 cm^{-1} and ten scans were coadded in 70 min of integration.

The system was calibrated with the vibration rotation lines of the impurity CO molecule near 2200 cm^{-1}. The absolute accuracy of the calibration is estimated to be $\pm$ 0.001 cm^{-1}. The precision of clear unblended C_3 lines is also about 0.001 cm^{-1}, but unfortunately, the spectrum was very congested. The precision of the line position measurements was, therefore, often degraded by the blending of lines.

III. ANALYSIS AND RESULTS

For the NRC measurements, the spectrum was recorded in the range between 6442 and 6529 cm^{-1}. The spectrum exhibited a beautiful triplet pattern as shown in Fig. 2 in the range between 6503 and 6529 cm^{-1}, and they became irregular and obscured below 6503 cm^{-1}. These transitions were thought to be R-branch transitions. The location of the band origin and the identification of the Q-branch lines were not obvious. The regular triplet pattern was not evident in the P-branch region. However, it was reasonable, from the beginning, to assume that the carrier of this spectrum was either C_3 or C_4, and judging from the line separations, C_3 was a more likely candidate.

Figures 3 and 4 present a closer picture of the triplet pattern of the R-branch lines. It was evident that the band exhibits a slight but significant staggering in the rotational

TABLE IV. Molecular constants of C_3 in lowest triplet states (in cm^{-1}).

	$\tilde{b}\ ^3\Pi_g$	$\tilde{a}\ ^3\Pi_u$
A	13.919 (44)[a]	13.556 (43)
B	0.424 524(22)	0.416 957(19)
$D\times10^6$	0.5755 (73)	0.368 (15)
$H\times10^{11}$	...	3.60 (43)
λ	0.0396 (73)	−0.0588 (68)
γ	−0.00222 (76)	−0.00461 (77)
o	0.581 (54)	0.595 (54)
$p\times10^3$	−2.2 (12)	−2.2 (12)
$q\times10^3$	0.174 (11)	0.377 (11)
T_v	6482.3903 (32)	...

[a] One standard error to the last digits of the quoted constants.

line spacing. This staggering can be understood by missing *e* or *f* components of the Λ-type doublets due to the spin statistics of equivalent ^{12}C nuclei. Therefore, the separation between the members of the *R*- or *P*-branch lines is about $2B$ rather than $4B$, and the possibility of C_4 was excluded. With the help of *ab initio* calculations, it was almost certain at this stage that the assignment of the band system was $\tilde{b}\,^3\Pi_g$–$\tilde{a}\,^3\Pi_u$. Figure 5 shows schematically the energy levels for both the upper and lower states. The parity or the *e* and *f* symmetry of the levels cannot be determined uniquely. In this analysis, we assumed the sign of the Λ-type doubling constant *o* to be positive.

The assignment of the F_1, F_2, and F_3 components were made considering the relative intensities of these components. The *J* numbering was difficult to make at the initial stage. After several trial and error procedures, we reached a reasonable assignment which is shown in Fig. 2.

A part of the Fourier-transform emission spectrum of C_3 is displayed in Fig. 4. The positions of the spectral lines were found by fitting each one to a Voigt profile with PC-DECOMP, a computer program developed at Kitt Peak, and this line list then used as input to PC-LOOMIS, an interactive color Loomis–Wood computer program, from which the F_1, F_2 and F_3 components could be picked out. An absolute *J* assignment for the components was facilitated by the many local perturbations to the upper state.

A least-squares analysis was carried out using an effective Hamiltonian derived by Brown and Merer.[38] The matrix elements calculated in terms of the case (a) basis set were given in Table I of Ref. 38. Numerous perturbations were found in the upper state. In the fit, the perturbed lines were excluded, and instead the combination differences for the

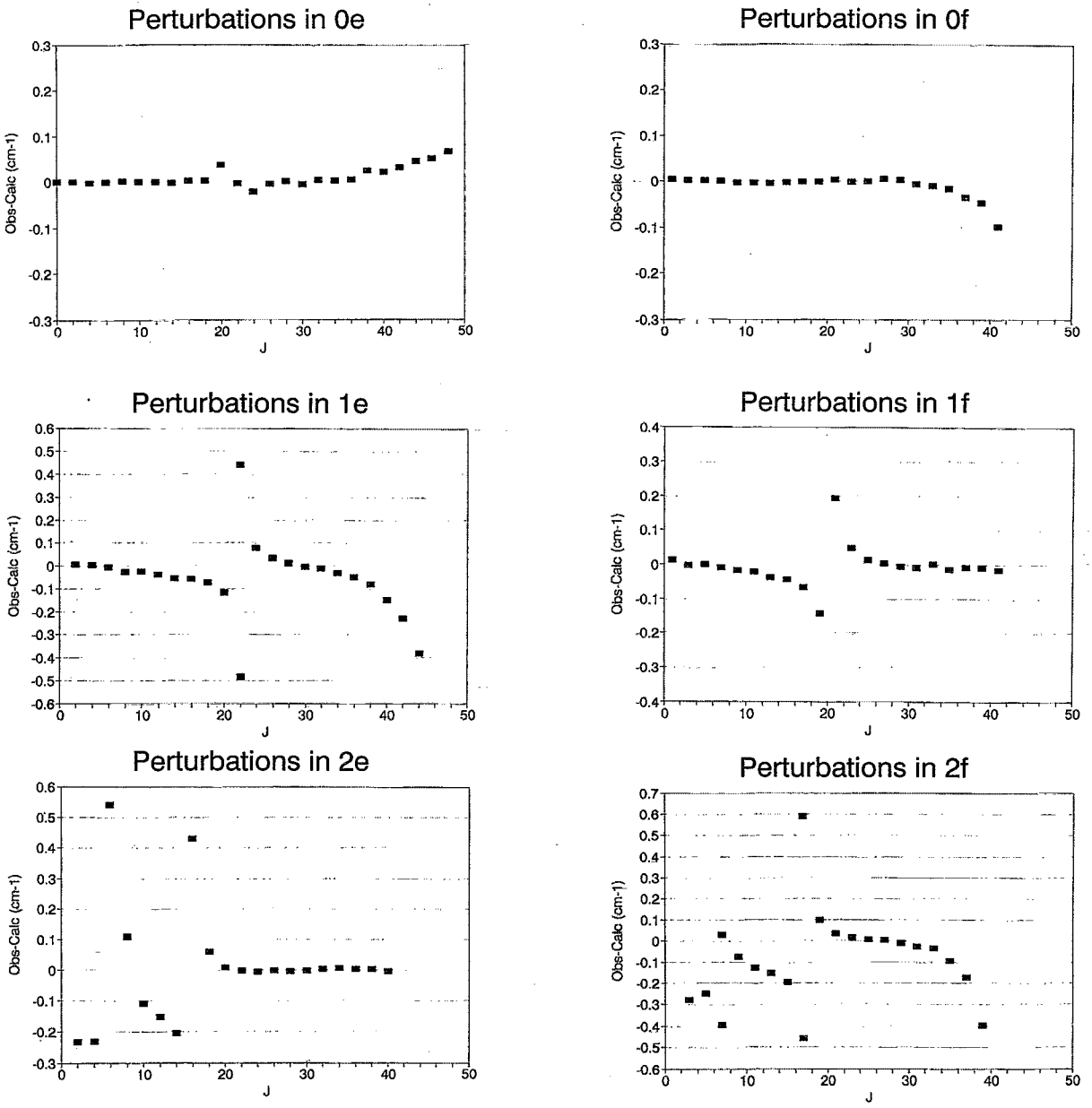

FIG. 6. Perturbations found in the upper state ($\tilde{b}\,^3\Pi_g$). (a) F_1 ($\Omega = 0$) *e* levels, (b) F_1 ($\Omega = 0$) *f* levels, (c) F_2 ($\Omega = 1$) *e* levels, (d) F_2 ($\Omega = 1$) *f* levels, (e) F_3 ($\Omega = 2$) *e* levels, and (f) F_3 ($\Omega = 2$) *f* levels.

lower state were included. Table II lists the lines assigned together with the deviations from the fit. The combination differences for the lower state are listed in Table III. Table IV lists the molecular constants determined from the fit. After we reached this assignment, we still cannot find several low-J lines of the F_3 components which are, presumably, strongly perturbed.

IV. DISCUSSION

The vibrational assignment of the band is not possible solely on the basis of the experiments reported here, but it is clear that neither of the states involve the bending vibration. If bending excitations were present, then a large Renner–Teller effect should be observed. There is little doubt that the lower state is the vibrational ground state. The upper state is also likely to be vibrationally unexcited, because the rotational constants in both two states are very similar, so only diagonal bands ($\Delta v_i = 0$) should have large Franck–Condon factors.

The r_0 bond length is calculated from the rotational constants to be 1.286 Å in $\tilde{b}\,^3\Pi_g$ and 1.298 Å in $\tilde{a}\,^3\Pi_u$. These values are to be compared with the r_0 bond length in the ground state (1.278 Å) and in the excited $\tilde{A}\,^1\Pi_u$ (1.305 Å). The $\tilde{a}\,^3\Pi_u$ and $\tilde{A}\,^1\Pi_u$ states arise from the same electron configuration. Therefore, it is very reasonable that the bond lengths in these states are very similar.

Figures 6(a)–6(f) show the deviations of the energies of the upper state levels obtained from the least-squares fit. Both the e and f components are perturbed similarly at similar J's; this suggests that a doubly degenerate (Π, Δ, Φ $\cdots$) state or states (probably a Π state) cause the perturbation rather than Σ states. The perturbing states are probably the excited vibrational states of the $\tilde{a}\,^3\Pi_u$ state. We observed complicated and congested features below 6460 cm^{-1}, which may be the (010)–(010) sequence band. This band will exhibit a complicated Renner–Teller effect. The Fourier-transform emission spectrum also contains a large number of unassigned features.

The spin–orbit coupling constants in the $\tilde{a}\,^3\Pi_u$ and $\tilde{b}\,^3\Pi_g$ are very similar. The unpaired electrons in the $\tilde{a}\,^3\Pi_u$ state occupy the $3\sigma_u$ and $1\pi_g$ orbitals, while in the $\tilde{b}\,^3\Pi_g$ state the $4\sigma_g$ and $1\pi_g$ orbitals are occupied. Only the π electron contributes to the diagonal spin–orbit interaction. Thus the spin–orbit constant A in these states should be very similar.

Among the fine structure constants, the spin–spin coupling constant λ is quite different in the upper and lower states. The λ constant is predominantly due to a second order contribution of the spin–orbit interaction. Therefore, it is sensitive to the locations of the interacting states. In contrast, Λ-type doubling constants are rather similar in both the states.

ACKNOWLEDGMENTS

H.S. gratefully acknowledges the Summit Post-Doctoral Fellowship for financial support for his trip and stay at National Research Council. We extend our appreciation to Dr. M. O'Sullivan for lending his mirrors which were essential in construction of the etalon. The National Solar Observatory is operated by the Association of Universities for Research in Astronomy, Inc., under contract with the National Science Foundation. C.J. and P.F.B. thank J. Wagner, R. Ram, and G. Ladd for assistance in acquiring our C_3 spectrum. Acknowledgment is made to the donors of the Petroleum Research Fund, administered by the American Chemical Society, for partial support of this work. Some support was also provided by the Astronautics Laboratory (Edwards Air Force Base) Grants No. F04611-87-K-0020 and F04611-90-K0031.

[1] W. Huggins, Proc. R. Soc. London **33**, 1 (1882).
[2] P. Swings, Rev. Mod. Phys. **14**, 190 (1942).
[3] A. McKellar, Astrophys. J. **108**, 453 (1948).
[4] G. Herzberg, Astrophys. J. **96**, 314 (1942).
[5] A. E. Douglas, Astrophys. J. **114**, 466 (1951).
[6] L. Gausset, G. Herzberg, A. Lagerqvist, and B. Rosen, Discuss. Faraday Soc. **1963**, 113.
[7] L. Gausset, G. Herzberg, A. Lagerqvist, and B. Rosen, Astrophys. J. **142**, 45 (1964).
[8] A. J. Merer, Can. J. Phys. **45**, 4103 (1967).
[9] G. W. Lemire, Z. Fu, Y. M. Hamrick, S. Taylor, and M. D. Morse, J. Phys. Chem. **93**, 2313 (1989).
[10] Eric A. Rohlfing, J. Chem. Phys. **91**, 4531 (1989).
[11] Eric A. Rohlfing and J. E. M. Goldsmith, J. Chem. Phys. **90**, 6804 (1989).
[12] F. J. Northrup and T. J. Sears, Chem. Phys. Lett. **159**, 421 (1989).
[13] R. L. Barger and H. P. Broida, J. Chem. Phys. **37**, 1152 (1962).
[14] W. Weltner, Jr., P. N. Walsh, and C. L. Angell, J. Chem. Phys. **40**, 1299 (1964).
[15] W. Weltner, Jr., and D. McDonald, Jr., J. Chem. Phys. **40**, 1305 (1964).
[16] W. Weltner, Jr., and D. McDonald, Jr., J. Chem. Phys. **45**, 3096 (1966).
[17] V. E. Bondybey and J. H. English, J. Chem. Phys. **68**, 4641 (1978).
[18] K. W. Chang and W. R. M. Graham, J. Chem. Phys. **77**, 4300 (1982).
[19] W. Weltner, Jr., and R. J. Van Zee, Chem. Rev. **89**, 1713 (1989).
[20] K. Matsumura, H. Kanamori, K. Kawaguchi, and E. Hirota, J. Chem. Phys. **89**, 3491 (1988).
[21] K. Kawaguchi, K. Matsumura, H. Kanamori, and E. Hirota, J. Chem. Phys. **91**, 1953 (1989).
[22] K. H. Hinkle, J. J. Keady, and P. F. Bernath, Science **241**, 1319 (1988).
[23] G. R. J. Williams, Chem. Phys. Lett. **33**, 582 (1975).
[24] J. Perić-Radić, J. Romelt, S. D. Peyerimhoff, and R. J. Buenker, Chem. Phys. Lett. **50**, 344 (1977).
[25] J. Romelt, S. D. Peyerimhoff, and R. J. Buenker, Chem. Phys. Lett. **58**, 1 (1978).
[26] Cary F. Chabalowski, J. Chem. Phys. **84**, 268 (1986).
[27] M. Rittby and R. Bartlett (to be published).
[28] K. K. Sunil, A. Orendt, K. D. Jordan, and D. DeFrees, Chem. Phys. Lett. **89**, 245 (1984).
[29] H. Sasada and T. Ohshima, J. Mol. Spectrosc. **136**, 250 (1989).
[30] H. Sasada and T. Amano, J. Chem. Phys. **92**, 2248 (1990).
[31] T. Amano and K. Tanaka, J. Chem. Phys. **83**, 3721 (1985).
[32] H. Sasada, S. Takeuchi, M. Iritani, and K. Nakatani, J. Opt. Soc. Am. B (submitted, 1990).
[33] R. S. Ram and P. F. Bernath, J. Mol. Spectrosc. **122**, 282 (1987).
[34] R. S. Ram and P. F. Bernath, J. Mol. Spectrosc. **122**, 275 (1987).
[35] P. F. Bernath, J. Chem. Phys. **86**, 4838 (1987).
[36] M. Douay, R. Nietmann, and P. F. Bernath, J. Mol. Spectrosc. **131**, 261 (1988).
[37] M. Douay, R. Nietmann, and P. F. Bernath, J. Mol. Spectrosc. **131**, 250 (1988).
[38] J. M. Brown and A. J. Merer, J. Mol. Spectrosc. **74**, 488 (1979).